View metadata, citation and similar papers at core.ac.uk
brought to you by CORE
provided by NASA Technical Reports Server

Uncertainty Evaluation of the Computational Model Used to Support the Integrated Powerhead Demonstrator Project

W.G. Steele[1], K.J. Molder[2], S.T. Hudson[3], K.V. Vadasy[4], P.T. Rieder[5], and T. Giel[6]

INTRODUCTION

NASA and the U.S. Air Force are working on a joint project to develop a new hydrogen-fueled, full-flow, staged combustion rocket engine [1]. The initial testing and modeling work for the Integrated Powerhead Demonstrator (IPD) project is being performed by NASA Marshall and Stennis Space Centers. A key factor in the testing of this engine is the ability to predict and measure the transient fluid flow during engine start and shutdown phases of operation. A model built by NASA Marshall in the ROCket Engine Transient Simulation (ROCETS) program is used to predict transient engine fluid flows. The model is initially calibrated to data from previous tests on the Stennis E1 test stand. The model is then used to predict the next run. Data from this run can then be used to recalibrate the model providing a tool to guide the test program in incremental steps to reduce the risk to the prototype engine. In our paper, we define this type of model as a calibrated model.

This paper proposes a method to estimate the uncertainty of a model calibrated to a set of experimental test data. The method is similar to that used in the calibration of experiment instrumentation. For the IPD example used in this paper, the model uncertainty is determined for both LOX and LH flow rates using previous data. The successful use of this model is then demonstrated to predict another similar test run within the uncertainty bounds. The paper summarizes the uncertainty methodology when a model is continually recalibrated with new test data. The methodology is general and can be applied to other calibrated models.

BACKGROUND

In general, modeling uncertainty exists due to numerical accuracy and simplifying assumptions and to variations in design conditions, input parameters, and other components of a model. Most of the literature on modeling uncertainty has addressed the effect of input parameter uncertainty. Some recent work has addressed the area of verification and validation (V&V) in an attempt to estimate the other components of model uncertainty.

The basis for modeling uncertainty was adapted from the widely used experimental uncertainty analysis. The experimental uncertainty analysis references for

[1] Mississippi State University, Mississippi State, MS
[2] Eglin Air Force Base, Eglin AFB, FL
[3] Drives & Controls Specialties, Hartsville, SC
[4] NASA Marshall Space Flight Center, MSFC, AL
[5] NASA Stennis Space Center, SSC, MS
[6] Sverdrup/ERC, Huntsville, AL

consisting of a transducer (t) and associated meter (m). Prior to calibration, the uncertainty of the instrumentation system (only considering the effects of the transducer and the meter, no measurement process effects) would be the root-sum-square of the transducer uncertainty and the meter uncertainty

$$u_{I_1} = \sqrt{u_t^2 + u_m^2} \tag{1}$$

where u is the standard uncertainty, an estimate of the standard deviation of the parent population of the error for each quantity. In the calibration process, a correction factor is added to the meter reading to make it match the value from the calibration standard system. This correction essentially replaces the uncertainty of the instrumentation system with the calibration (c) system uncertainty so that

$$u_{I_2} = u_c \tag{2}$$

The calibration system uncertainty will be the root-sum-square of the systematic (fixed) standard uncertainty of the calibration standard, b_{c_1} the systematic standard uncertainty of the calibration standard meter, b_{c_2}, (if a different meter is used for the standard from that used for the transducer), and any random standard uncertainty in the calibration process, s_c, so that

$$u_c = \sqrt{b_{c_1}^2 + b_{c_2}^2 + s_c^2} \tag{3}$$

The systematic standard uncertainty b is a standard deviation level estimate of the possible distribution of fixed errors, and the random standard uncertainty is the standard deviation of the calibration correction [5]. If the same meter is used for the calibration standard and the transducer, then the b_{c_2} term would not be included in Equation 3.

Usually, a calibration is done over a range, and a curve-fit (cf) is performed to develop a relationship between the meter reading and the calibrated output value. The curve-fit will not give an exact correction for all meter readings; therefore, there will be an additional uncertainty in the calibrated instrumentation system output because of the curve-fit error. Often, the effects of this error are estimated as a standard error of regression for the curve-fit [4]. The instrumentation uncertainty is then

$$u_{I_3} = \sqrt{u_c^2 + u_{cf}^2} \tag{4}$$

The uncertainty u_{I_3} takes into account the calibration correction for the transducer and the meter and includes the curve-fit uncertainty. In some cases, the meter used in testing (m_2) is different from the meter used in calibration (m_1). Changing the meter requires that the systematic standard uncertainties of both meters be included in the instrumentation system uncertainty

a standard error of regression, or it can be an uncertainty estimate that varies over the range of the simulation results, whichever is appropriate. For the calibrated model, the simulation uncertainty in Equation 6 is replaced by the root-sum-square of the data uncertainty, u_d, and the comparison error uncertainty, u_E, so that

$$u_{s_1} = \sqrt{u_d^2 + u_E^2} \tag{8}$$

The uncertainty in Equation 8 would apply for simulation results over the range of the input parameter values used in the calibration of the model with the assumption that the input parameters have the same uncertainties that they had in the calibration process (the same transducers are used for input readings or the same source is used for input data). Often, the input parameters used in a simulation calculation from a calibrated model will be from different sources or transducers from those used in the calibration process. These different sources will also have associated uncertainties that are independent of the original parameter uncertainties. This case is similar to changing the meter in the instrumentation calibration, and the uncertainties from both sets of input parameters would have to be included in the simulation uncertainty

$$u_{s_2} = \sqrt{u_d^2 + u_E^2 + u_{sp_1}^2 + u_{sp_2}^2} \tag{9}$$

The uncertainties u_{sp_1} and u_{sp_2} would be evaluated using Equation 7 taking into account only the parameters that changed sources between the calibration and the calculation of the new simulation result.

The development above is for the general case of a calibrated model. In the next section, a specific example is given for the IPD testing being done by NASA and the U.S. Air Force.

IPD EXAMPLE

Experimental Data

The experimental data used in this study was activation data. Activation is the process through which a facility is tested and checked for problems before a test article is installed. The facility included the liquid oxygen (LOX) and liquid hydrogen (LH2) run tanks to supply the test liquids and the supply piping from the tanks to the test article interface. The supply piping included the venturis to measure the mass flow rates and many other purge valves and bleed valves. A pneumatically controlled butterfly valve was used to represent the IPD test article at the test article interface during the activation tests. The run tanks from which the test liquids flowed kept a near constant pressure throughout each test. Therefore, the butterfly valves controlled the flow for each system.

The parameters of interest for this study are the LOX system mass flow rate and the LH2 system mass flow rate of the IPD activation tests. Both of these flow rates are measured by their respective venturi flow meters. The venturi flow rate, WPUMP, used

Table 1. Input Parameter Uncertainty Summary

Parameter	Units	LOX Uncertainty	LH2 Uncertainty
C_d	NA	.00488	.00484
F	NA	negligible	negligible
D_T	inches	.001 inches	.001 inches
D_I	inches	.01 inches	.01 inches
ρ	lb_m/ft^3	1.0%	1.0%
ΔP	psid	1.21 psi	1.21 psi

Table 2. Venturi Mass Flow Rate Uncertainty Summary

LN Flow Rate	Uncertainty (%)	LOX Flow Rate	Uncertainty (%)	LH2 Flow Rate	Uncertainty (%)
.76+	1.70	.93+	2.00	.89+	2.80
.68 -.76	1.90	.84 -.93	2.10	.78 -.89	3.30
.59 -.68	2.10	.76 -.84	2.40	.67 -.78	3.90
.51 -.59	2.40	.68 -.76	2.60	.55 -.67	4.40
.42 -.51	2.90	.59 -.68	3.00	.44 -.55	5.50
.34 -.42	3.50	.51 -.59	3.50	.33 -.44	7.80
.25 -.34	4.70	.42 -.51	4.10	.22 -.33	11.1
.17 -.25	7.30	.34 -.42	5.10	.11 -.22	22.2
.12 -.17	10.1	.25 -.34	6.80	.09 -.11	29.9
.10 -.17	11.8	.17 -.25	10.6	.07 -.09	37.7
		.15 -.17	11.5	.04 -.07	55.5
				.02 -.04	110.9

A schematic of the IPD activation system modeled in this study is given as Figure 1. The overall ROCETS scheme is an iterative, multi-variable, Newton-Rahpson predictor-corrector equation solver. It starts with initial pressure and enthalpy guesses at the nodes to determine all needed fluid properties. Properties are defined at nodes (circles in Figure 1), not in the legs connecting nodes. Then ROCETS calculates flows and flow derivatives in each leg from the leg's resistance value and fluid density. Next ROCETS predicts new node pressures and enthalpies to conserve mass, momentum, and energy within each volume. Newton-Rahpson iteration is performed to solve the set of the mass, momentum, and energy equations imbedded in the flow and volume modules representing the different system components. Iteration on the corrector continues at each time step until convergence to within a preselected tolerance of the variables is reached. If convergence is not attained within a preselected number of steps, the time step is reduced and iteration begins anew. Pressures, enthalpies, flow rates, etc., are determined at each time step in this manner to get to a solution.

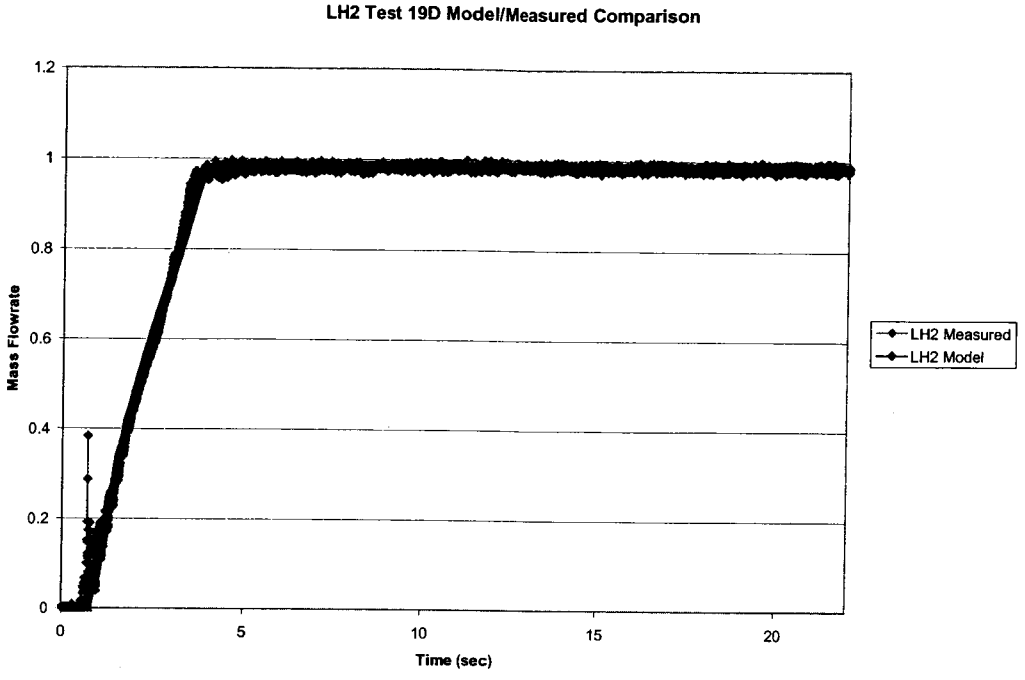

Figure 2. LH2 Test 19D Model/Measured Comparison

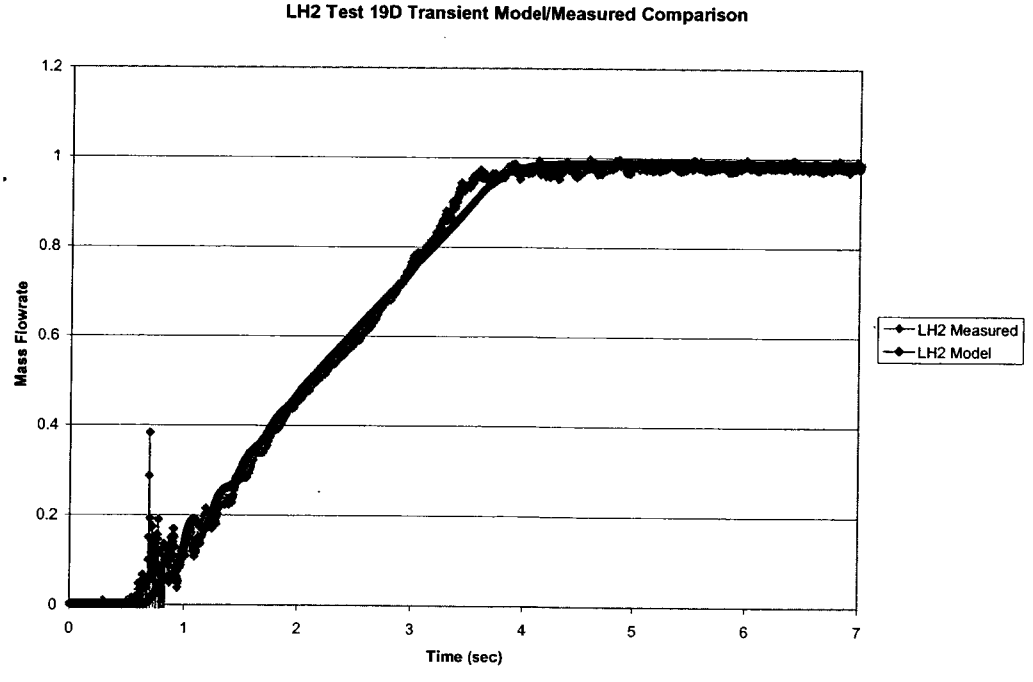

Figure 3. LH2 Test 19D Transient Model/Measured Comparison

Simulation Uncertainty

Since this IPD activation test model is used to predict future test conditions at slightly higher flow rates with the same input data measurements, the simulation uncertainty is determined using Equation 8. Therefore, the simulation uncertainty at a 95% confidence level, U_s, is determined as

$$U_s = 2\sqrt{u_d^2 + u_E^2} \qquad (12)$$

The data uncertainty will be the same as the calibration uncertainty given in Equation 3, the root-sum-square of the systematic and random standard uncertainties for the data. The flow rate data had oscillating flow as seen in Figures 2-5, but there was negligible random uncertainty in these IPD activation tests. The systematic uncertainties, $2b_d$, for the flow rate data is given in Table 2; therefore, for these tests u_d will be one-half of these tabulated values and will vary with the predicted flow rate.

For these tests, the difference between the calibrated model values and the data in Figures 2-5 was taken as 95% confidence estimates of u_E. The comparison uncertainty varies with time for each test. The values are smaller during the initial low-flow and final high-flow steady-state regions of the test and are larger during the transient regions.

The calibrated model was used to predict two additional runs, LOX test 9B and LH2 test 19A. Both of these tests were similar in setup and duration to the calibration data. Test 9B used liquid nitrogen in the LOX system while LH2 was again used in the LH2 system. The LOX system test durations were approximately 20 seconds, and the LH2 system tests were approximately 60 seconds. The start-up region is time 5-7 seconds for the LOX system and time 0-7 seconds for the LH2 system.

The model was run with the simulation uncertainty applied, and the model was compared to the data with the data uncertainty included. The plots of the full run for the LH2 system are given in Figures 6, 7, and 8. Figure 6 displays the full range of the uncertainty for the simulation and data. The flow rate uncertainty was over 100 % before the transient section because the ΔP measurements of the venturi were very low in the low-flow range. Plotting the LH2 modeling with a more reasonable scale that does not include unrealistic values less than zero gives Figure 7. The LH2 system transient section is displayed in Figure 8. The plots of the full run for the LOX system are given in Figures 9, 10, and 11. Figure 9 shows that flow rate uncertainty was over 100 % in the low-flow range because, as in the LH2 system, the ΔP measurements of the venturi for the LOX system were very low. Figure 10 plots the data with a more reasonable scale that does not include unrealistic values less than zero. The transient section is given in Figure 11.

The comparison run LH2 system test data fell within the predicted uncertainty bands for the model. The only point for which this was not true was the beginning of the high-flow steady-state section of the test. This was due to a phenomenon in the test that was not recorded in the data. The difference between the actual and predicted mass flow rate in this region of the test was deemed to not have an adverse effect on the operation of the engine. Therefore, it was not considered a constraint to engine testing and was not investigated further. However, it was suggested that the cause could be from slight

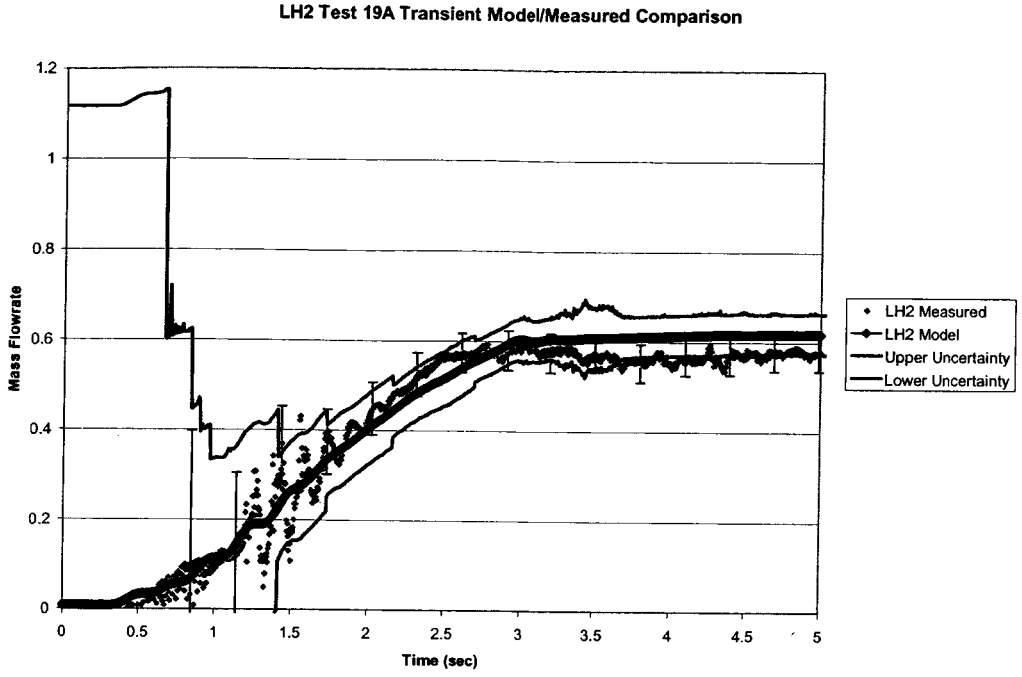

Figure 8. LH2 Test 19A Transient Model/Measured Comparison with Uncertainty

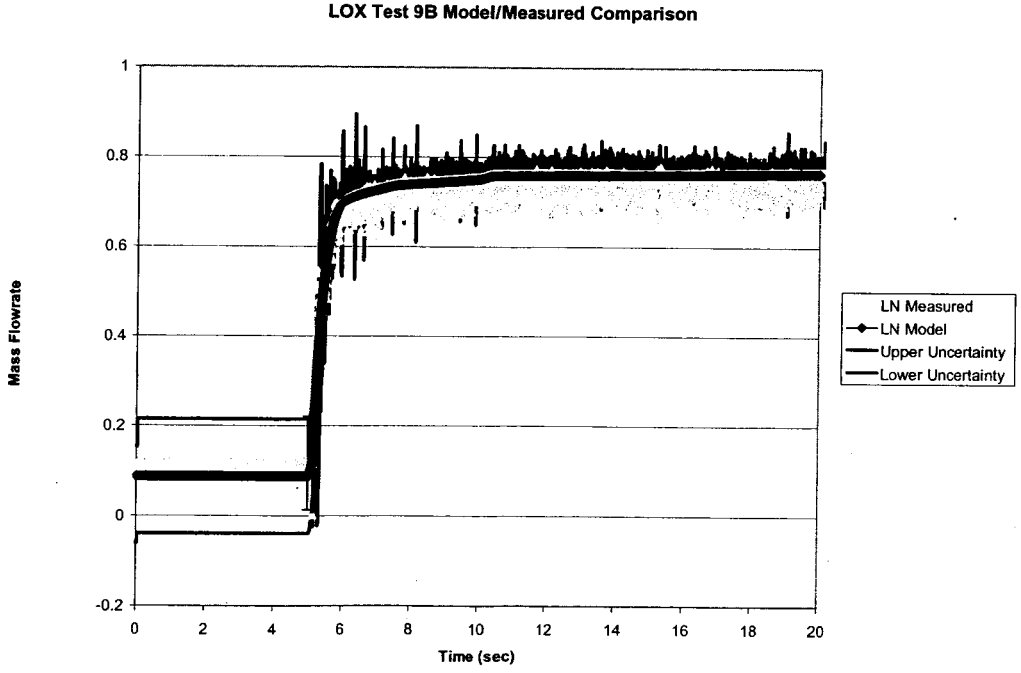

Figure 9. LOX Test 9B Model/Measured Comparison with Uncertainty Full Range

The comparison run LOX system test data did not fall within the predicted uncertainty bands for the model as well as the LH2 data did. The data covers the lower uncertainty band shown in the steady state section of the test. This problem was most likely due to LN being used as the test liquid instead of LOX. The model was calibrated with LOX as the fluid, and the comparison model used LN as the fluid with no changes made to the model to account for fluid viscosity changes which would produce leg resistance changes. This caused a higher simulation flow rate than was measured. However, the general shape of the test data was matched. It is expected that the comparison would have been better if LOX had been used as the test liquid. Although, even with the different fluid, the difference between the simulation results and the data for the high-flow steady-state region was about 8 % as compared to the simulation uncertainty of 5 %. Also, this difference should not be a problem for calibrated modeling since ROCETS models are only calibrated with different fluids in the early, low-flow rate stage of development and not in the later stages which require low simulation uncertainties.

CONCLUSIONS

A method to determine the simulation uncertainty of a calibrated model was developed. The Coleman and Stern [13] model validation process was adapted to help formulate the simulation uncertainty methodology required. This methodology was then applied to the model when it was used to predict additional test results.

The uncertainty analysis of the experimental data was done using methodology described in Coleman and Steele [5]. The uncertainty of the experimental data was essentially the uncertainty of the venturi flow meters used to measure the mass flow rate. This uncertainty was dominated by the ΔP measurement of the venturi. The uncertainty of the venturi was acceptable during the transient and high flow rate steady-state regions of the tests. However, at low flow rates before the transient section began, the uncertainty was over 100 %. This was due to the ΔP measurement being very low. To correct this problem at the lower flow rates a pressure transducer with a smaller range would be needed [14].

Comparison error between the calibrated model and the calibration data was used as a way to quantify the comparison uncertainty associated with the simulation. These uncertainties in conjunction with the venturi uncertainty were the two components of the overall simulation uncertainty. The comparison uncertainty was large during the transient regions and small during the steady-state regions.

The process of calibrating a model each time new data is available is logical for the work that is done at NASA Stennis test facilities. Due to the fact that no two engine test series are the same, making one model to encompass all possibilities is impractical. The model uncertainty methodology in this study fits this process of a calibrated model that is constantly "tweaked." This tweaking leaves the user with a calibrated model that can be used to predict the next test condition. A comparison of the model prediction and the next run then shows if additional corrections (calibration) need to be made and how reliable the model predictions should be for future safe engine operation.

[13] Coleman, H. W. and Stern, F., "Uncertainties and CFD Code Validation," Journal of Fluids Engineering, Vol. 119, 1997, pp. 795-803.

[14] Hudson, S. T., Steele, W. G., Ryan, H. M., Hughes, M. S., and Hammond, J. M., "Test Facility Uncertainty Analyses for RBCC Systems Testing," AIAA Paper 2002-3607, 38th AIAA Joint Propulsion Conference, Indianapolis, IN, July 7-10, 2002.

[15] Seymour, D. C., ROCETS User's Manual, Space Transportation Directorate, Marshall Space Flight Center, 1999.